$12^{th}$ International Conference on Fracture Mechanics of Concrete and Concrete Structures
FraMCoS-12
B.L.A. Pichler, Ch. Hellmich, P. Preinstorfer (Eds)

https://doi.org/10.21012/FC12.1204
MS17-1:1

# THE EFFECT OF CORROSION RATE ON CORROSION-INDUCED CRACKING IN REINFORCED CONCRETE

**EVŽEN KOREC[1,3*], MILAN JIRÁSEK[2], HONG S. WONG[1] AND EMILIO MARTÍNEZ-PAÑEDA[3]**

[1]Department of Civil and Environmental Engineering, Imperial College London, Exhibition Road, London SW7 2AZ, United Kingdom, e.korec20@imperial.ac.uk, hong.wong@imperial.ac.uk

[2]Department of Mechanics, Faculty of Civil Engineering, Czech Technical University in Prague, Thákurova 7, Prague 166 29, Czech Republic, milan.jirasek@cvut.cz

[3]Department of Engineering Science, University of Oxford, Oxford OX1 3PJ, UK, emilio.martinez-paneda@eng.ox.ac.uk

**Key words:** Reinforced concrete, Corrosion-induced cracking, Impressed current testing

**Abstract.** Corrosion of steel in concrete is responsible for 70-90% of the premature deterioration of reinforced concrete structures and can even cause structural failure, as infamously documented by the recent collapse of aerated concrete panels in the UK. Under field conditions, corrosion of reinforced concrete is a slow process that takes years or decades. Therefore, high corrosion rates are artificially applied in laboratory conditions to shorten the duration of experiments. It has been known for decades that this underestimates the damage caused by corrosion under natural conditions, but the reasons for this have been unclear. Based on recent experimental results, we propose a hypothesis that explains this phenomenon by the variability of the chemical composition of rust, in particular the variable ratio of iron oxides and iron hydroxy-oxides, with the applied corrosion rate. The simulation results obtained were found to be able to reproduce the hitherto puzzling trends in the experimental data for different corrosion rates. The proposed model can be used to estimate the error caused by the acceleration of corrosion tests and to extrapolate the results to the natural corrosion regime.

## 1 INTRODUCTION

This study deals with the mathematical modelling of corrosion-induced cracking in reinforced concrete. Concrete is the second most used material in the world after water. However, 70-90% of reinforced concrete structures deteriorate prematurely due to corrosion of the steel reinforcement embedded in the concrete [1, 2]. This leads to significant damage or even sudden structural collapse, as illustrated by the recent failures of reinforced autoclaved aerated concrete (RAAC) panels [3], which forced the closure of more than 100 schools in England. Corrosion-induced cracking is a dominant degradation mechanism, leading to the fracture of the concrete cover and its subsequent delamination or spalling, exposing the embedded steel members to the elements. As natural corrosion in concrete is a long-term process, lasting years or decades, experimental investigation of naturally corroding specimens alone is not feasible. For this reason, researchers often resort to impressed current testing, which can significantly accelerate corrosion-induced cracking. This is achieved by applying a high corrosion current density in hundreds or thousands of $\mu\mathrm{A}/\mathrm{cm}^2$, drastically reducing the duration of the experiment to days or hours.

Although the impressed current technique is very time-efficient, it raises the applied current density well above the range of values typical for natural corrosion (about 1 $\mu\mathrm{A}/\mathrm{cm}^2$ [4, 5, 6, 7, 8]). This raises the question of whether the crack propagation rate (understood, for example, as the rate of surface crack width in relation to the thickness of the uniformly corroded rust layer) resulting from impressed current tests is representative of corrosion in field conditions. Several studies have investigated this problem and found that accelerating the corrosion current up to about 200 $\mu\mathrm{A}/\mathrm{cm}^2$ resulted in significantly slower crack propagation (with respect to the same thickness of corroded rust layer) [9, 10, 11, 12, 13]. For example, Alonso and Andrade [12] reported that the slope of the linearly fitted crack width/corrosion penetration curve for the corrosion rate of 10 $\mu\mathrm{A}/\mathrm{cm}^2$ was even six times greater than for the corrosion rate of 100 $\mu\mathrm{A}/\mathrm{cm}^2$.

While the decrease in crack propagation rate with increasing corrosion rate is well-documented, there is no agreement on the origin of this phenomenon. Pedrosa and Andrade [13] suggested that the loading rate-dependent material properties of concrete may be responsible. If true, this would effectively mean that the effect of corrosion rate on crack propagation rate is due to concrete creep. While creep is likely to affect the results of long-term tests conducted under natural-like corrosion current densities, an extensive modelling study by Aldellaa et al. [14] concluded that creep alone does not explain the dependence of the crack propagation rate on the corrosion rate.

To elucidate the interplay between corrosion rate and crack propagation rate, we propose a new hypothesis [15] that relates the chemical composition of rust, in particular the ratio of iron oxides and iron hydroxy-oxides, to the applied corrosion rate. We further propose that the variable chemical composition affects the density of the rust so that the pressure on the concrete, and hence the induced crack propagation rate, decreases with increasing current density. This assumption is adopted in a coupled chemo-mechanical model that we have previously proposed [15]. It is shown that the simulation results obtained reproduce the hitherto puzzling decreasing trend of the crack propagation rate with increasing corrosion current density.

## 2 THE IMPACT OF CORROSION RATE ON THE CHEMICAL COMPOSITION OF RUST

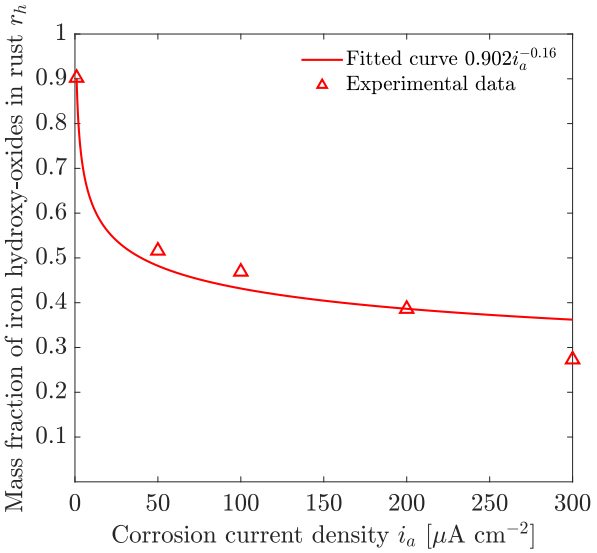


Figure 1: The mass fraction of hydroxy-oxides rust $r_h$ with varying corrosion current densities. While the content of hydroxy-oxides is high for corrosion under natural conditions (corrosion current densities around 1 $\mu\mathrm{A}/\mathrm{cm}^2$), it decreases rapidly with increasing corrosion rate applied in impressed current tests.

To study the effect of corrosion rate on the chemical composition of the rust, we assume that corrosion is initiated and progresses uniformly over the steel surface with a constant corrosion current density $i_a$. This is a typical scenario for impressed current tests. As the electric current flows, $\mathrm{Fe}^{2+}$ ions are released from the steel surface into the pore solution. Prior to rust formation, the dissolved iron ions form a number of intermediate products (see Refs. [16, 17, 18, 19, 20] for more details). Although there are many types of rust, X-ray diffraction (XRD) measurements have shown that regardless of the corrosion rate, the main

corrosion products are iron oxides (wüstite $\mathrm{FeO}$, hematite $\alpha-\mathrm{Fe_2O_3}$, magnetite $\mathrm{Fe_3O_4}$) and iron hydroxy-oxides (goethite $\alpha-\mathrm{FeO(OH)}$, akaganeite $\beta-\mathrm{FeO(OH)}$, lepidocrocite $\gamma-\mathrm{FeO(OH)}$, ferroxyhite $\delta-\mathrm{FeOOH}$) [21, 22, 23, 24, 25, 26]. It should be noted that the XRD method can only determine the presence of crystalline materials, but some corrosion products are known to be amorphous [21].

Crucially for this study, there is experimental evidence that the mass ratio of iron oxides and iron hydroxy-oxides varies with the applied corrosion rate. The experimental data of Zhang et al. [24], depicted in Fig. 1, indicate that the mass ratio $r_h$ of iron hydroxy-oxides is as high as 0.9 when corrosion proceeds under natural conditions, i.e. with a current density of about 1 $\mu\mathrm{A/cm^2}$ [4, 5, 6, 7, 8]. However, $r_h$ decreases dramatically with corrosion rate to about 0.5 for 50 $\mu\mathrm{A/cm^2}$, while a subsequent decrease is much more moderate. In Fig. 1, the data of Zhang et al. [24] are fitted with a power function $k_1(i_a/i_{a,ref})^{k_2}$ where $i_{a,ref}=1$ $\mu\mathrm{A/cm^2}$ is the reference corrosion current density. Except for the first data point on the left in Fig. 1, Zhang et al. [24] measured the content of iron oxides and iron hydroxy oxides in controlled corrosion rate tests. However, the first data point was from a naturally corroding sample for which the corrosion rate was not known. Thus, we estimated the corrosion rate to be 1 $\mu\mathrm{A/cm^2}$, which is a typical value measured during the natural corrosion process in reinforced concrete [4, 5, 6, 7, 8]. Although experimental measurements of the mass ratio of specific corrosion products are very rare in the current literature, the results of Zhang et al. [24] are in agreement with studies on samples corroded under natural conditions [23, 22] and with accelerated impressed current tests [27]. The ratio of iron oxides to iron hydroxy-oxides in the rust has a profound impact on the overall density of the rust and therefore the pressure exerted on the concrete by the rust accumulation under confined conditions. While the molar volume ratio of iron oxide rust to iron is about 2, it increases to about 3 for iron hydroxy-oxide rust. This results in a significantly increased corrosion-induced pressure on the concrete when the content of hydroxy-oxides in the rust is high.

## 3 THE CHEMO-MECHANICAL MODEL FOR CORROSION-INDUCED CRACKING

To investigate the effect of the corrosion rate on the crack propagation rate, we have used a chemo-mechanical model described in detail in our previous study [15]. The state-of-the-art knowledge of the underlying processes has been incorporated into three interrelated sub-models – (i) a reactive transport model for the transport of iron ions released from the steel surface into the concrete pore space where they precipitate as rust, (ii) a model for the corrosion-induced pressure resulting from the simultaneous constrained accumulation of compressible rust in (ii.A) the dense rust layer in the steel volume vacated by corrosion and (ii.B) in the concrete pore space (evaluated with a newly proposed precipitation eigenstrain), and (iii) a phase-field fracture model of Wu et al. [28, 29] calibrated to accurately describe the quasi-brittle fracture of concrete. The proposed model was implemented in COMSOL Multiphysics software and solved numerically using the finite element method.

## 4 RESULTS

The geometry and mechanical properties of the simulated impressed current tests were adopted from the study of Pedrosa and Andrade [13] (see detailed discussion of the chosen parameter values in our previous study [15]). Fig. 2a depicts a typical fracture pattern obtained from numerical simulations. The main crack propagates over the shortest distance between the concrete surface and the rebar, perpendicular to the concrete surface, and opens wide with the ongoing corrosion process. In addition, two other lateral cracks form. For the same corrosion penetration, i.e. the thickness of the corroded steel layer $t_{cor}$, the crack width decreases with increasing applied corrosion current den-

sity (see Fig. 2b), as observed in experimental studies [12, 13, 30, 9, 31, 32, 11]. In the proposed model, this behaviour results from the hypothesis that the chemical composition of rust, in particular the mass ratio of iron oxides and iron hydroxy-oxides, changes with the magnitude of the applied current density (see Fig. 1), such that the rust density increases with increasing current density, reducing the pressure caused by constrained expansion.

To analyse the effect of corrosion rate on crack propagation rate, series of identical impressed current tests were simulated at varying current density. The predicted crack width $w$ was fitted linearly by $w = \beta t_{cor} + \zeta$. This allowed the crack width slope $\beta$ to be compared with its experimental counterpart measured by Pedrosa and Andrade [13], who applied the same fitting procedure to their experimentally measured crack widths. Only the crack widths $w \geq 1$ µm was considered in the fitting to avoid the bias caused by non-linearity for zero and very small crack widths. The linear fit was found to be quite accurate for the thinner concrete of 20 mm (Fig. 2b). However, for the thicker cover of 40 mm, the crack width increases superlinearly with $t_{cor}$, which makes the linear fit less accurate. For the thicker concrete cover, the predicted crack width slope $\beta$ is therefore affected by the maximum evaluated $t_{cor}$ and the linear fit is not optimal.

Comparison of the predicted crack width slope $\beta$ with the experimental data from [13] shows that the predictions are within the experimental range and accurately reproduce the observed trend, such that the slope $\beta$ decreases with a negative power of the current density [13]. To assess how well the predictions match this trend, the results were fitted using $\beta = \gamma_1 (i_a / i_{a,ref})^{\gamma_2}$ where $i_{a,ref} = 1$ µA/cm$^2$ is the reference corrosion current density. As shown in Fig. 3, the predictions for a 20 mm concrete cover show excellent agreement with this model. However, for the thicker 40 mm cover, the results are more scattered, although the overall trend is still consistent. There are two reasons for this behaviour.

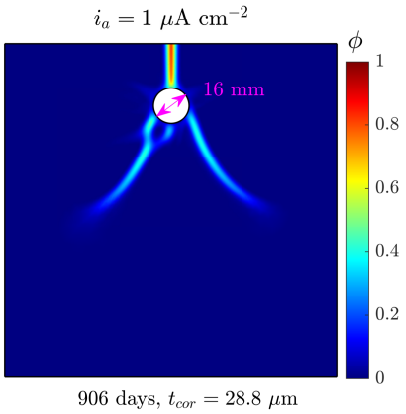


(a)

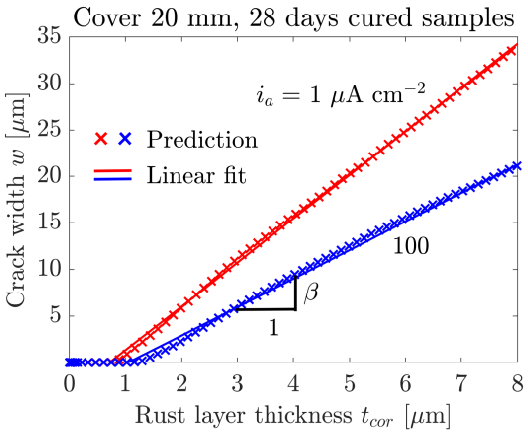


(b)

Figure 2: (a) Corrosion-induced cracks in a uniformly corroding reinforced concrete specimen resolved by the phase-field fracture method. The phase field variable $\phi = 1$ indicates a fully cracked sample while $\phi = 0$ denotes undamaged concrete. For this simulation, the 28-days old concrete, the concrete cover of 20 mm and the corrosion current of $i_a = 1$ µA/cm$^2$ were considered. (b) The surface crack width of the crack between the rebar and the upper concrete surface increases with time with the thickness of the corroded steel layer $t_{cor}$. For identical $t_{cor}$, $w$ decreases with increasing applied current density as a result of the changing chemical composition of the rust, which causes its density to increase and thus the corrosion-induced pressure to decrease.

Firstly, for thicker concrete cover, the crack width/corrosion penetration curve is non-linear

and therefore a linear fit is not optimal. Secondly, it has been observed that as the concrete cover thickness increases, the model becomes numerically more sensitive, leading to slight variations in the surface crack width due to small numerical differences. These differences influence the formation of specific crack patterns, resulting in varied crack width evolution.

The proposed model is able to capture the initially rapid decrease of $\beta$ with increasing current density $i_a$, as indicated by the experimental data of Pedrosa and Andrade [13]. For current densities above about 50 $\mu\mathrm{A}/\mathrm{cm}^2$, the rate of decrease of $\beta$ becomes more gradual. As shown in Fig. 3, this trend is in good qualitative agreement with the experimental observations. However, for current densities below 10 $\mu\mathrm{A}/\mathrm{cm}^2$, the slopes reported by Pedrosa and Andrade [13] are significantly larger than those predicted by the simulations. While the study by Pedrosa and Andrade [13] remains the most thorough experimental investigation of the effect of impressed current magnitude on crack width slope, it involved a limited number of specimens (11 in total), with each test performed only once. Thus, it is not clear whether the observed discrepancy between the quantitative values of the numerical predictions and the experiments is due to the experimental error or to some other phenomena not accounted for by the model. Clearly, more extensive experimental campaigns are needed. For current densities greater than 10 $\mu\mathrm{A}/\mathrm{cm}^2$, the numerical predictions are in better quantitative agreement with the experimental measurements, although they mostly underestimate the experimental values.

The comparison of data for four scenarios—two curing times (resulting in different mechanical properties) and two concrete cover thicknesses—depicted in Fig. 3 shows that $\beta$ increases with longer curing times, resulting in improved mechanical properties. In addition, a thicker concrete cover can result in a higher $\beta$ at lower, natural current densities. This was observed in the case of a 40 mm cover combined with 147 days curing, consistent with our previous findings [33]. The modelling results in Fig. 3 suggest that the influence of concrete cover thickness is considerably more significant than curing time (and hence concrete strength). Furthermore, the effect of curing time on $\beta$ diminishes as the current density increases.

Understanding the slope of crack width with respect to corrosion penetration under natural conditions is critical to accurately predicting the duration of the corrosion propagation period, i.e. the time between corrosion initiation and critical delamination or spalling of the concrete cover. Currently, national design codes estimate durability based on the time to corrosion initiation, which is governed by the diffusion of aggressive agents such as chlorides from the concrete surface to the steel reinforcement. However, this approach is overly conservative because, while corrosion initiation is often the longest phase, the propagation time can also be significant. For example, results for a 40 mm thick concrete cover and 28 days cured concrete indicate that under natural conditions (typically $i_a \leq 1$ $\mu\mathrm{A}/\mathrm{cm}^2$) the propagation period could be at least 7 years before a surface crack width of 0.3 mm (the Eurocode limit for serviceability) is reached. However, even this threshold may underestimate the time to severe delamination or spalling, as noted in [12, 34].

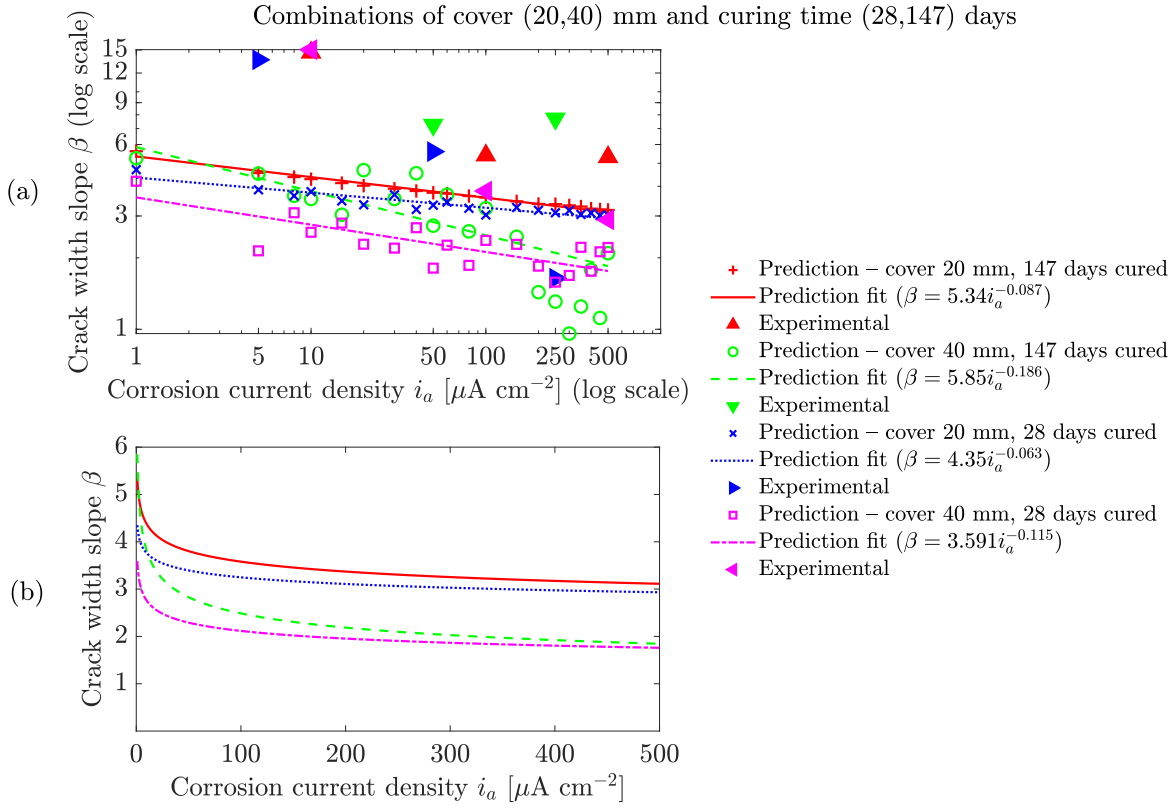


Figure 3: The slope $\beta$ of the linearly fitted predicted crack width ($w = \beta t_{cor} + c$) for varying current density $i_a$ is shown in (a) and (b). The slope $\beta$ decreases with increasing current density. In the log-log plot (a) it can be observed that the model captures well the decreasing negative power-law trend of the crack width slope with current density. However, the experimental results depicted in (a) suggest even higher slopes for lower current densities such as $i_a = 5$ µA/cm$^2$. In figure (b) it is easier to observe the rapid decrease of the crack width slope $\beta$ up to about $i_a = 50$ µA/cm$^2$. This is followed by a more moderate decrease.

## 5 CONCLUSIONS

This study examines the effect of the corrosion rate applied in impressed current tests on the crack propagation rate, which has puzzled researchers for nearly three decades. A new hypothesis has been proposed that relates the chemical composition of rust, in particular the mass ratio of its major constituents, iron oxides and iron hydroxy-oxides, to the impressed current density applied. This hypothesis was implemented in our recently proposed phase-field-based chemo-mechanical model for corrosion-induced cracking in reinforced concrete, and numerical simulations were validated with available experimental studies. The main findings are summarised as follows:

- The simulation results strongly support the hypothesis that the chemical composition of rust changes with increasing corrosion current density. This would explain the experimentally observed slower crack growth (relative to corrosion penetration) in accelerated impressed current tests compared to natural conditions [12, 13, 30, 9, 31, 32, 11, 9].

- The simulations support the experimental conclusion of Pedrosa and Andrade [13] that the decay of the slope of the crack width as a function of corrosion penetration follows a negative power law of the corrosion current density.

- Current design codes estimate corrosion resistance as the time to corrosion initiation (determined by the diffusion of aggressive agents such as chlorides through the concrete cover). This approach is overly conservative as it neglects the propagation phase (from corrosion initiation to significant delamination/spalling). Incorporating the propagation stage into the service life predictions can significantly extend the service life estimates. For example, for a 40 mm concrete cover and 28 days cured concrete, the proposed model predicts that under natural conditions ($i_a \leq 1$ $\mu\mathrm{A/cm^2}$) it would take at least 7 years to reach a surface crack width of 0.3 mm.

Overall, the proposed framework allows computational impressed current testing to complement experimental studies and to estimate the error due to artificial corrosion acceleration. While the simulation results strongly support the hypothesis that rust composition changes with corrosion current density, further experimental studies are essential to confirm this conclusively. In addition, the exact chemical mechanisms driving these composition changes remain to be elucidated.

## 6 ACKNOWLEDGEMENTS

The authors would like to express their gratitude to Prof Carmen Andrade (CIMNE International Center for Numerical Methods in Engineering, Barcelona) for her invaluable advice and stimulating discussions. E. Korec acknowledges financial support from the Imperial College President's PhD Scholarships. M. Jirásek acknowledges financial support from the European Union under the ROBOPROX project [grant no. CZ.02.01.01/00/22_008/0004590]. E. Martínez-Pañeda was supported by an UKRI Future Leaders Fellowship [grant MR/V024124/1]. We additionally acknowledge computational resources and support provided by the Imperial College Research Computing Service (http://doi.org/10.14469/hpc/2232).

## References

[1] C. Gehlen et al. *Fib Bulletin 59 - Condition control and assessment of reinforced concrete structures exposed to corrosive environments (carbonation/chlorides)*. fib - The International Federation for Structural Concrete, 2011. ISBN: 978-2-88394-099-4.

[2] A. E. K. Jones and B. K. Marsh. *Development of an holistic approach to ensure the durability of new concrete construction*. British Cement Association (BCA), 1997, p. 81. ISBN: 9780721015224.

[3] P. Ball. “When the roof falls in”. In: *Nature Materials* 22.10 (2023), p. 1162.

[4] M. Otieno, H. Beushausen, and M. Alexander. “Prediction of corrosion rate in reinforced concrete structures - A critical review and preliminary results”. In: *Materials and Corrosion* 63.9 (2012), pp. 777–790.

[5] M. Otieno, H. Beushausen, and M. Alexander. “Chloride-induced corrosion of steel in cracked concrete - Part I: Experimental studies under accelerated and natural marine environments”. In: *Cement and Concrete Research* 79 (2016), pp. 373–385.

[6] C. Andrade. “Steel corrosion rates in concrete in contact to sea water”. In: *Cement and Concrete Research* 165 (2023), p. 107085.

[7] M. T. Walsh and A. A. Sagüés. “Steel corrosion in submerged concrete structures-part 1: Field observations and corrosion distribution modeling”. In: *Corrosion* 72.4 (2016), pp. 518–533.

[8] C. Andrade. “Role of Oxygen and Humidity in the Reinforcement Corrosion”. In: *Proceedings of the 75th RILEM Annual Week 2021: Advances in Sustainable Construction Materials and Structures*. Cham, Switzerland: Springer, 2023, pp. 316–325.

[9] K. Vu, M. G. Stewart, and J. Mullard. “Corrosion-induced cracking: Experimental data and predictive models”. In: *ACI Structural Journal* 102.5 (2005), pp. 719–726.

[10] M Saifullah and L. A. Clark. “Effect of corrosion rate on the bond strength of corroded reinforcement”. In: *Corrosion and corrosion protection of steel in concrete* 1 (1994), pp. 591–602.

[11] J. A. Mullard and M. G. Stewart. “Corrosion-induced cover cracking: New test data and predictive models”. In: *ACI Structural Journal* 108.1 (2011), pp. 71–79.

[12] C. Alonso et al. “Factors controlling cracking of concrete affected by reinforcement corrosion”. In: *Materials and Structures* 31.211 (1996), pp. 435–441.

[13] F. Pedrosa and C. Andrade. “Corrosion induced cracking: Effect of different corrosion rates on crack width evolution”. In: *Construction and Building Materials* 133 (2017), pp. 525–533.

[14] I. Aldellaa et al. “Effect of creep on corrosion-induced cracking”. In: *Engineering Fracture Mechanics* 264 (2022), p. 108310.

[15] E. Korec et al. “Unravelling the interplay between steel rebar corrosion rate and corrosion-induced cracking of reinforced concrete”. In: *Cement and Concrete Research* 186 (2024), p. 107647.

[16] E. Wieland et al. “Speciation of iron(II/III) at the iron-cement interface: a review”. In: *Materials and Structures* 56.2 (2023), pp. 1–24.

[17] O. X. Leupin et al. “Anaerobic corrosion of carbon steel in bentonite: An evolving interface”. In: *Corrosion Science* 187 (2021), p. 109523.

[18] F. E. Furcas et al. “Solubility and speciation of iron in cementitious systems”. In: *Cement and Concrete Research* 151 (2022), p. 106620.

[19] F. E. Furcas et al. “Speciation Controls the Kinetics of Iron Hydroxide Precipitation and Transformation at Alkaline pH”. In: *Environmental Science & Technology* 58.44 (2024), pp. 19851–19860. ISSN: 0013-936X, 1520-5851.

[20] M. Stefanoni et al. “The kinetic competition between transport and oxidation of ferrous ions governs precipitation of corrosion products in carbonated concrete”. In: *RILEM Technical Letters* 3 (2018), pp. 8–16.

[21] Y. Zhao et al. “Composition and expansion coefficient of rust based on X-ray diffraction and thermal analysis”. In: *Corrosion Science* 53.5 (2011), pp. 1646–1658.

[22] A. Köliö et al. “Corrosion products of carbonation induced corrosion in existing reinforced concrete facades”. In: *Cement and Concrete Research* 78 (2015), pp. 200–207.

[23] W. J. Chitty et al. “Long-term corrosion resistance of metallic reinforcements in concrete - A study of corrosion mechanisms based on archaeological artefacts”. In: *Corrosion Science* 47.6 (2005), pp. 1555–1581.

[24] W. Zhang, J. Chen, and X. Luo. “Effects of impressed current density on corrosion induced cracking of concrete cover”. In: *Construction and Building Materials* 204 (2019), pp. 213–223.

[25] Q. Liu et al. “In-situ deformation modulus of rust in concrete under different levels of confinement and rates of corrosion”. In: *Construction and Building Materials* 255 (2020), p. 119369.

[26] E. Sola et al. “Experimental and numerical study of accelerated corrosion of steel reinforcement in concrete: Transport of corrosion products”. In: *Cement and Concrete Research* 120 (2019), pp. 119–131.

[27] X. Zhang et al. “Corrosion induced stress field and cracking time of reinforced concrete with initial defects: Analytical modeling and experimental investigation”. In: *Corrosion Science* 120 (2017), pp. 158–170.

[28] J.-Y. Wu. “A unified phase-field theory for the mechanics of damage and quasi-brittle failure”. In: *Journal of the Mechanics and Physics of Solids* 103 (2017), pp. 72–99.

[29] J.-Y. Wu. “Robust numerical implementation of non-standard phase-field damage models for failure in solids”. In: *Computer Methods in Applied Mechanics and Engineering* 340 (2018), pp. 767–797.

[30] P. S. Mangat and M. S. Elgarf. “Strength and serviceability of repaired reinforced concrete beams undergoing reinforcement corrosion”. In: *Magazine of Concrete Research* 51.2 (1999), pp. 97–112.

[31] K. A. Vu and M. G. Stewart. “Predicting the Likelihood and Extent of Reinforced Concrete Corrosion-Induced Cracking”. In: *Journal of Structural Engineering* 131.11 (2005), pp. 1681–1689.

[32] T. A. El Maaddawy and K. A. Soudki. “Effectiveness of Impressed Current Technique to Simulate Corrosion of Steel Reinforcement in Concrete”. In: *Journal of Materials in Civil Engineering* 15.1 (2003), pp. 41–47.

[33] E. Korec et al. “A phase-field chemo-mechanical model for corrosion-induced cracking in reinforced concrete”. In: *Construction and Building Materials* 393 (2023), p. 131964.

[34] C. Andrade, C. Alonso, and F. J. Molina. “Cover cracking as a function of bar corrosion: Part I-Experimental test”. In: *Materials and Structures* 26.8 (1993), pp. 453–464.